Optics Communications 282 (2009) 1913–1917

Contents lists available at ScienceDirect

Optics Communications

journal homepage: www.elsevier.com/locate/optcom

Manifestations of sub- and superluminality in filamented femtosecond laser pulse in fused silica

Ivan Blonskyi [a], Viktor Kadan [a,*], Oleh Shpotyuk [b], Igor Dmitruk [a]

[a] Dept. of Photonic Processes, Institute of Physics NAS of Ukraine, 46 Prospekt Nauky, Kyiv 03680, Ukraine
[b] Scientific Research Company "Carat", 202, Stryiska Str., Lviv 79031, Ukraine

ARTICLE INFO

Article history:
Received 23 October 2008
Received in revised form 23 January 2009
Accepted 23 January 2009

PACS:
42.65.Re
42.65.Jx
52.38.Dx

Keywords:
Femtosecond laser pulses
Kerr effect
Filaments
Superluminality

ABSTRACT

Filamented propagation of femtosecond laser pulses in fused silica is studied using microscopy of Femtosecond Time-resolved Optical Polarigraphy (FTOP). Both super- and subluminal translation of axial intensity maxima in a 100 fs time scale has been directly recorded. The observed spatio-temporal periodicity of the pulse shape in longitudinal and transversal directions is tentatively interpreted as two projections on *X* and *Y* axes of the same fringe pattern formed by the interference of the axial part of the beam and spontaneously generated conical beam.

1. Introduction

If the power of laser pulse traveling in fused silica exceeds critical value P_{cr} (1.9 MW or 0.33 μJ energy at 150 fs pulse duration at $\lambda = 780$ nm and nonlinear Kerr refractive index $n_2 = 3.2 \times 10^{-16}$ cm^2/W), then self-focusing occurs resulting in filament formation [1,2]. A remarkable property of the filament propagation is superluminal motion of the filament intensity maximum. Recording of this phenomenon is interesting both from fundamental and practical points of view, e.g. generation of THz radiation is attributed to Cherenkov emission from superluminal movement of ionization front [3]. Superluminal propagation of the filament core follows from the earliest moving focus model [2] and is an inherent property of monochrome conical or Bessel-X-wave [4]. For the Bessel wave $v_g \approx v_p = c/n \cdot \cos\theta$, where v_g – group velocity of the conical wave packet, v_p – its phase velocity; c – light velocity in vacuum, n – refraction index of the medium, θ – the angle between the propagation axis and the wave vectors of the conical wave packet. The superluminality of v_p in that case follows from the simple geometric examination of movement of conical wave fronts. The same is also valid for the generalized X-wave, which is composed of a polychromatic conical wave packet with wavelength dependent θ, thus providing the properties of difractionlessness and stationarity. Group velocity exceeding that of light of the axicon formed Bessel beam was observed in argon in an experiment monitoring the propagation of ionization front [5]. So far, the superluminal behavior of femtosecond filaments was experimentally recorded only in air in an indirect experiment on filament concatenation [6], demonstrating advance of about 100 fs of filamented pulse over the nonfilamented one. However, direct observations of superluminality in spontaneously formed femtosecond filaments, particularly in solids, to the best of our knowledge are still absent. Spontaneous generation of the Bessel-type conical beam in initially Gaussian filamented beam caused by Kerr focusing and nonlinear losses was experimentally demonstrated and simulated in a number of works [7–9]. The latest experimental and numerical investigation of space–time dynamics of ultrashort laser pulse propagating in water [10] suggests formation of shock front on both trailing and leading edges of the pulse caused by formation of the subluminal and superluminal intensity peaks.

In the present work, we have conducted a study of the spatio-temporal propagation dynamics of filamented femtosecond laser pulse in fused silica using FTOP. In addition to the direct recording of superluminal translations of the pulse maximum, we reveal

* Corresponding author. Tel./fax: +380 44 5251543.
E-mail addresses: kadan@iop.kiev.ua, vikkadan@yahoo.com (V. Kadan).

0030-4018/$ - see front matter © 2009 Elsevier B.V. All rights reserved.
doi:10.1016/j.optcom.2009.01.056

correlation between the longitudinal and transversal spatial periodicities of the pulse shape.

2. Experimental

Among various experimental methods [2], FTOP [11,12] directly visualizes propagating light itself, allowing the space–time mapping of induced Kerr birefringence. General scheme of the experiment is shown in Fig. 1. Regenerative amplifier 1 generates a train of 2.5 mJ, 150 fs, 780 nm, 1 kHz, horizontally polarized pulses. The $\lambda/2$ retarder plate 5 and the Glan prism 6 produce vertically polarized pump beam of adjustable power. Variable aperture 7 cuts out the narrower beam before it enters the objective 8 with focal position inside the $3 \times 3 \times 50$ mm polished sample 10, made of KU-1 brand of fused silica of the former Soviet Union, at 1.5 mm depth from the front surface and 0.3 mm from the left-side surface. The sample 10 was fixed on a 3D translation stage with motorized *Z*-axis and was translated vertically with 50 μm/s velocity during the measurements. The aperture diameter 1.8 mm and pump pulse energy 2.9 μJ (after the aperture inside the sample) were chosen to produce a single filament inside the bulk of silica. Objective 9 images the filament on a 1200×1600 matrix of monochrome CCD-camera with 4.4×4.4 μm pixel size and 0.4 μm/pixel scale with 2 μm spatial resolution. Variably delayed probe beam serves as a flash for time-resolved photos. Axis of the film polarizer 11 was set at 45° to the vertical position. Axis of the polarizer 12 is also set at 45° but in the crossed position relative to polarizer 11. The pump pulse induces instant birefringence in the fused silica due to the Kerr effect, $n_e - n_o$ being $I_{pump} \cdot n_2$, where I_{pump} – pump intensity. The area with induced birefringence acts as a phase retarder, making polarization of the probe light to be elliptical. The polarization component orthogonal to the big axis of the ellipse survives the second polarizer 12, producing FTOP signal. For small phase shifts, intensity of the FTOP signal after analyzer 12 can be written as [13] $I_{FTOP} = \pi^2 d^2 n_2^2 I_{pump}^2 I_{probe}/\lambda_{probe}^2$, where d denotes the pump–probe interaction length, I_{probe} – probe light intensity, and λ_{probe} – probe wavelength,. Thus, I_{FTOP} represents instantaneous pump intensity distribution. According to a more explicit expression for the FTOP image, given in [14] the spatial intensity distribution is determined by convolution of the probe signal and the square of integral of intensity of the pump signal along the interaction direction *Y*. Therefore, when interpreting FTOP images, one should take into account the following factors: (i) non-zero probe duration causes blur along the propagation axis (actually, FTOP photo is a convolution of the pump and probe pulses); (ii) $I_{FTOP} \propto I_{pump}^2$; (iii) actually, I_{pump} is space-dependent, so the full I_{FTOP} signal is an integral of I_{pump} along the interaction direction.

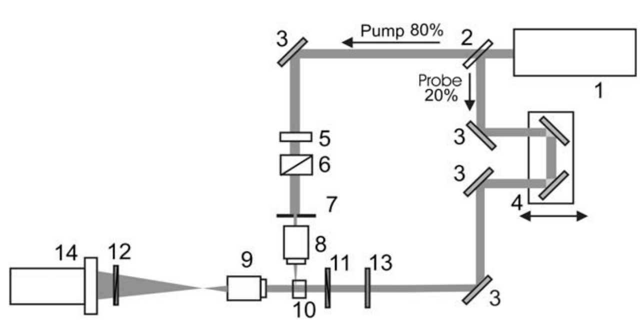

Fig. 1. General scheme of the experimental setup: 1 – femtosecond regenerative amplifier; 2 – splitting mirror; 3 – bending mirrors; 4 – delay line; 5 – $\lambda/2$ retarder plate, 6 – Glan prism; 7 – variable aperture; 8, 9 – microscopic objective 10×, 0.25NA; 10 – fused silica sample; 11, 12 – film polarizer; 13 – gray attenuator filter; 14 – CCD-camera.

3. Experimental results and discussion

We have taken 33 FTOP photos with 100 fs delay increment, covering 640 μm propagation distance. Zero delay $\tau = 0$ corresponds to the photo # 1. To avoid saturation of the CCD-matrix the exposure time *T* varied during the measurements in the following way: $T = 1$ s for $0\ \text{ps} \geqslant \tau \geqslant 0.6$ ps; $T = 0.2$ s for $0.7\ \text{ps} \geqslant \tau \geqslant 1.2$ ps; $T = 0.5$ s for $1.3\ \text{ps} \geqslant \tau \geqslant 3.2$ ps. In Fig. 2 fifteen consecutive FTOP images are presented with 0.2 ps delay increment, beginning from $\tau = 0.2$ ps (a) to $\tau = 3.0$ ps (o). The laser pulse travels from left to right along the *X* axis. Photos (a) and (b) show the pulse positions before the transition to the filamented mode. The FWHM of the transverse profile of IFTOP1/2 in (a) is 12 μm, and that of the longitudinal profile is 46 μm. In assumption of Gaussian temporal profile for the laser pulse, this value closely corresponds to the measured pulse duration of 150 fs, accounting the convolution expansion by the factor 0.625 and using the value $n = 1.45$ for refraction index of fused silica. Gradual decrease of the beam diameter caused by self-focusing is observed when τ increases from 0 to 0.5 ps. No transformation of the longitudinal beam profile occurs in this delay interval. In (c), partial transition to the filament mode is recorded, FWHM being 3 μm at the front edge and 8 μm at the trailing one. The role of self-focusing at this transition to the filamented propagation mode is clear, among others, from the fact, that the theoretical diffraction limit of the focal spot diameter for the microscope objective used is 11 μm for 1.8 mm beam. The transition to the filamented mode is accompanied also by longitudinal elongation of the pulse profile, probably indicating its temporal splitting, which can not be resolved in our measurements due to the long duration of the probe pulse. Axial intensity profiles of the FTOP signal, taken for a narrow selection area of 2 μm wide

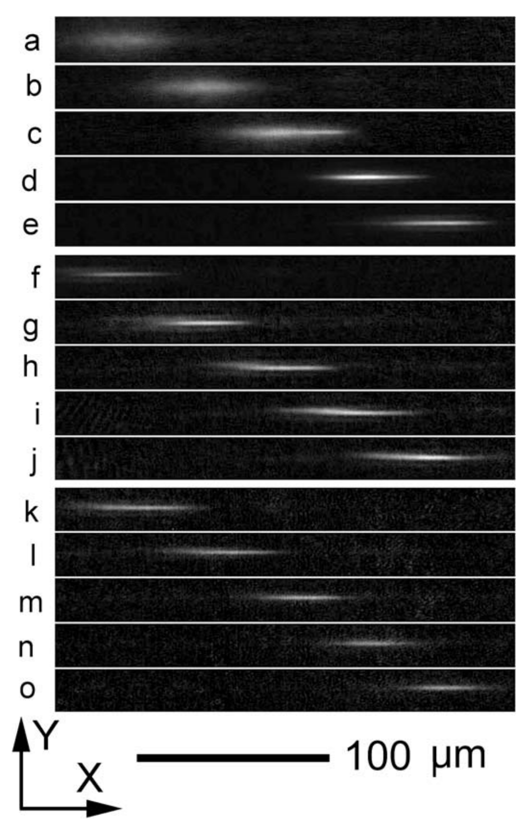

Fig. 2. FTOP images at increasing delay. (a–c) CCD exposure time $T = 1$ s, (d–f) $T = 0.2$ s, (g–o) $T = 0.5$ s. Time delay τ in picoseconds is 0.2 (a), 0.4 (b), 0.6 (c), 0.8 (d), 1.0 (e), 1.2 (f), 1.4 (g), 1.6 (h), 1.8 (i), 2.0 (j), 2.2 (k), 2.4 (l), 2.6 (m), 2.8 (n), 3.0 (o). The *X* range is kept the same within every group of five photos (a–e), (f–j), and (k–o).